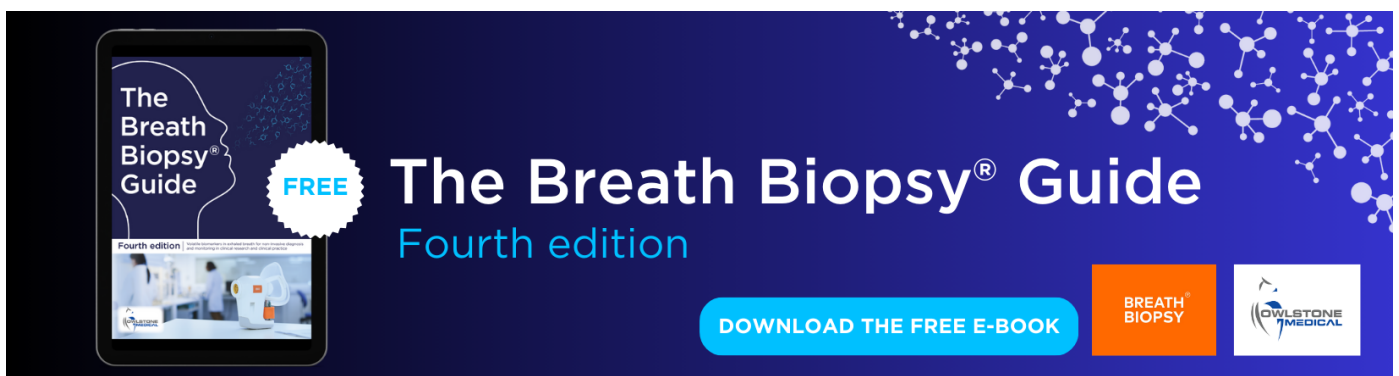**LETTER • OPEN ACCESS**

Disentangling physical and dynamical drivers of the 2016/17 record-breaking warm winter in China

To cite this article: Tuantuan Zhang *et al* 2022 *Environ. Res. Lett.* **17** 074024

View the article online for updates and enhancements.

ENVIRONMENTAL RESEARCH
LETTERS

LETTER

Disentangling physical and dynamical drivers of the 2016/17 record-breaking warm winter in China

Tuantuan Zhang[1,2] (iD), Yi Deng[3], Junwen Chen[4,*] (iD), Song Yang[1,2], Peng Gao[5] and Henian Zhang[3]

[1] School of Atmospheric Sciences, Sun Yat-sen University, Southern Laboratory of Ocean Science and Engineering, Zhuhai, Guangdong 519082, People's Republic of China
[2] Guangdong Province Key Laboratory for Climate Change and Natural Disaster Studies, Sun Yat-sen University, Zhuhai, Guangdong 519082, People's Republic of China
[3] School of Earth and Atmospheric Sciences, Georgia Institute of Technology, Atlanta, GA 30319, United States of America
[4] Shenzhen Wiselec Technology Co., Ltd, Shenzhen, Guangdong 518048, People's Republic of China
[5] Meteorological Bureau of Liupanshui, Liupanshui, Guizhou 553001, People's Republic of China
* Author to whom any correspondence should be addressed.

E-mail: junwen.chen@wiselec.cn

Abstract

Understanding the physical and dynamical origin of regional climate extremes remains a major challenge in our effort to anticipate the occurrences and mitigate the adverse impacts of these extremes. China was hit by a record-breaking hot winter in 2016/17 with remarkable surface warming over the northern and southeastern regions. Here we made a quantitative attribution of this 2016/17 winter's surface temperature anomalies utilizing an updated version of the coupled atmosphere-surface climate feedback response analysis method (CFRAM), that recently incorporates the effect of aerosols and more species of trace gases (CFRAM-A). The CFRAM-A analysis reveals that the overall warming pattern may be largely attributed to the effects of anomalous water vapor, atmospheric dynamics, and aerosols, followed by anomalies of surface albedo, clouds, solar irradiance, ozone, and carbon dioxide. The effect of methane turns out to be negligible. Anomalies in surface dynamics provides an overall cooling effect, compensating the warming associated with other processes to some extent. Among the three major positive contributors, effects of water vapor and atmospheric dynamics prevail over both northern and southeastern China while the impact of anthropogenic aerosols appears much more pronounced over southeastern China, likely due to the implementation of highly effective emission reduction policies in China since 2013. The CFRAM-A thus provides an efficient, model-free approach for quantitatively understanding sources of regional temperature extremes and for assessing the impacts of environmental policies regulating anthropogenic emissions of aerosols and atmospheric trace gases.

1. Introduction

According to the Sixth Assessment Report of the Intergovernmental Panel on Climate Change (IPCC AR6), global surface temperature during the most recent decade (2011–2020) was approximately 1 °C higher than 1850–1900, and extreme warm events became more frequent and more intense across most continents. Attribution of the climate warming or specific extreme events, a process of quantifying and evaluating the relative contributions from multiple causal factors, provides an important scientific basis for policymakers and stakeholders to formulate mitigation and adaptation strategies (Lashof and Ahuja 1990, Stott *et al* 2010, Hegerl and Zwiers 2011, Zhai *et al* 2018). In spite of remarkable progresses made so far in attribution studies, there is still a long way before we can obtain attribution results with low uncertainties (Rodhe 1990, Liebmann *et al* 2010, Najafi *et al* 2015, Qian and Zhang 2019). While

insufficiency and imperfection of observational data is one of the factors to blame, limitations of existing attribution methods also contribute significantly to uncertainties in results obtained. To date, attribution studies rely primarily on sensitivity experiments conducted with climate models, which often lead to large uncertainties in quantitative results due to considerable model biases (Gu *et al* 2006, Hegerl and Zwiers 2011, Turnock *et al* 2015, Zhai *et al* 2018, Gong *et al* 2021).

The coupled atmosphere-surface climate feedback response analysis method (CFRAM) has proven to be an efficient off-line diagnostic tool that can directly decompose local temperature differences between two climate states into partial temperature changes associated with individual radiative and dynamical processes (Cai and Lu 2009, Lu and Cai 2009). This method has been successfully applied to quantify the relative contributions of multiple processes to temperature anomalies associated with global warming (Chen *et al* 2017a, 2017b, Hu *et al* 2018), El Niño-Southern Oscillation (Deng *et al* 2012, Park *et al* 2012, Hu *et al* 2016), and the Northern Annular Mode (Deng *et al* 2013), etc. Nevertheless, a fly in the ointment is that the effect of aerosols, which is a key factor for temperature changes through aerosol-cloud-radiation interaction (Giorgi *et al* 2002, Li *et al* 2007, Jiang *et al* 2015), has not been included in the previous CFRAM analysis. Scientists basically reached an agreement on the qualitative effects of aerosols, but quantifying the contribution of aerosols to temperature change remains technically challenging for the attribution community (Ruckstuhl *et al* 2010, Turnock *et al* 2015, Yang *et al* 2016).

As a region experienced rapid population growth, urbanization, and industrial development in the past century, China has become the major sources of anthropogenic aerosols around the world (Liao *et al* 2014, Li *et al* 2015). In order to achieve the reduction of particulate matter concentrations by 10%–25% in the year 2017 with respect to the 2013, the Action Plan on the Prevention and Control of Air Pollution was launched in 2013 with strengthened reduction of anthropogenic emissions across China (Zheng *et al* 2018, Filonchyk *et al* 2019, Fang *et al* 2020). Such human interventions would introduce both uncertainties and complexities to quantitative attribution studies.

Owing to the limited observations and complex climate conditions, attribution studies of climate changes and extreme events remain inadequate in China (Zhai *et al* 2018). The nation-wide extreme warm winter will facilitate glacier retreat, snow melt, and degradation of permafrost over the Tibetan Plateau (Yao *et al* 2019, Zhang *et al* 2019a, Duan *et al* 2022), favor the serve haze events in eastern China (Cai *et al* 2017, Yin *et al* 2017), affect winter wheat

production (Tian *et al* 2012, Zhang *et al* 2021), and disturb the ecosystems (Yu *et al* 2010, Zhang *et al* 2019c). The long-term increase of warm winters over China are favored by the global warming (Sun *et al* 2021), while the interannual variability of winter temperature is regulated by the atmospheric internal variabilities (e.g. the Siberian High, Arctic Oscillation, the East Asian winter monsoon) and external forcings (e.g. El Niño–Southern Oscillation, Arctic sea ice, North Atlantic sea surface temperature, Indian Ocean sea surface temperature; You *et al* 2013, Jiang *et al* 2014, Zuo *et al* 2015, 2022, Ma *et al* 2018, Xiao *et al* 2018, Xie *et al* 2019). The attribution research of extreme warm winter in China are relatively scarce. Jian *et al* (2020) and Pan *et al* (2021) investigated the roles of sea surface temperature anomalies and the East Asian winter monsoon in two regional extreme warm winters over China. However, the relative contributions of multi factors have not been comprehensively quantified. Recently, a record-breaking hot winter hit China in 2016/17, with the national averaged surface temperature nearly 2 °C higher than the 2005–2019 climatology (figure 1(a)). Until now, causal factors responsible for this extreme warm winter remain unknown. Based on the Modern-Era Retrospective Analysis for Research and Application, version 2 (MERRA-2) with long-term coupled meteorological and aerosol analysis, and an updated version of the CFRAM that innovatively includes the aerosol effect (CFRAM-A hereafter), this study provides a comprehensive and quantitative attribution of individual physical and dynamical processes for the surface temperature anomalies over China in the 2016/17 winter.

2. Data and methods

The CFRAM-A developed in this study is based on the total energy balance in an atmosphere-surface column consisting multi atmospheric layers and one surface layer (Cai and Lu 2009, Lu and Cai 2009). Taking the difference (Δ) of the total energy balance equation between two climate states (climate '*B*' minus '*A*'), and linearizing the radiative energy perturbations by neglecting the interactions among different radiative species, we may express ΔS (*S* denotes the convergence of shortwave radiation flux) and (*R* denotes the divergence of longwave radiation flux) as the sum of partial radiative energy flux convergence/divergence due to individual processes. Multiplying both sides by the inverse of the Planck feedback matrix $\left(\frac{\partial R}{\partial T}\right)^{-1}$, which quantifies the change of the vertical profile of longwave radiative flux divergence due to 1 K warming (with respect to the climate state '*A*' temperature) at an atmospheric or surface layer, and rearranging the terms (details referred to Chen *et al* 2017a), we obtain:

$$\Delta T = \left(\frac{\partial R}{\partial T}\right)^{-1} \begin{bmatrix} \Delta S^{(SR)} + \Delta(S-R)^{(CO_2)} + \Delta(S-R)^{(CH_4)} + \Delta(S-R)^{(CLD)} + \Delta S^{(AL)} + \\ \Delta(S-R)^{(WV)} + \Delta(S-R)^{(O_3)} + \Delta(S-R)^{(BC)} + \Delta(S-R)^{(OC)} + \\ \Delta(S-R)^{(SULF)} + \Delta(S-R)^{(SS)} + \Delta(S-R)^{(DUST)} + \Delta Q^{(atmos\_dyn)} + \Delta Q^{(surf\_dyn)} \end{bmatrix}, \quad (1)$$

where ΔT are the temperature differences between the two climate states in each layer. The convergence of total non-radiative energy due to changes in atmospheric dynamics $\Delta Q^{(atmos\_dyn)}$ and surface dynamics $\Delta Q^{(surf\_dyn)}$ is estimated as a residual from the radiative energy perturbations. The vertical profile of the temperature difference at a given location between two climate states could be decomposed into the vertical profile of partial temperature differences due to (from left to right in equation (1)) changes in solar irradiance, CO_2, CH_4, cloud, surface albedo, water vapor, ozone, black carbon, organic carbon, sulfate, sea salt, dust, atmospheric dynamics (i.e. energy transport by convective and large-scale atmospheric motions), and surface dynamics (including mainly energy gain in the column due to surface latent and sensible heat fluxes, runoff, soil heat diffusion, and snow/ice melting/freezing). Note that methane (CH_4) is the second most abundant anthropogenic greenhouse gas after carbon dioxide (CO_2). It has greenhouse effect, i.e. trapping the longwave radiation in the atmosphere, which is the same as CO_2. The linearization of radiative perturbations by omitting the higher order terms of the interactions among different species (e.g. water vapor, clouds, aerosols) has been extensively validated and is now commonly adopted in many climate attribution methods (e.g. partial radiative perturbation method) in numerous studies (e.g. Wetherald and Manabe 1988, Bony *et al* 2006, Held and Soden 2006, Taylor *et al* 2011). Note that the partial temperature changes associated with aerosols are results from the direct radiative effects (i.e. cool the surface by reducing surface incoming sunlight). On the other hand, the energy perturbations due to the changes in clouds indeed include the indirect effects of aerosols.

The rapid radiative transfer method (RRTM) for general circulation model (RRTMG) is an accelerated version of RRTM with minimal loss of accuracy (Iacono *et al* 2008), which has been evaluated and widely employed in many state-of-the-art climate models and weather models. The RRTMG version 5 is incorporated into the CFRAM-A to obtain the individual radiative energy perturbations in equation (1) by conducting off-line radiative transfer calculations separately for climate state 'A' ('base state') and multiple perturbed state 'B's associated with different physical processes. The aerosol optical properties (e.g. absorption, extinction, single-scatter albedo, and asymmetry parameter) for the five types of aerosols are from the four-mode version of the modal aerosol model (MAM4; Liu *et al* 2016) in the Community Atmosphere Model version 6.3 (CAM6). The Monte Carlo integration of the independent column approximation (McICA; Pincus *et al* 2003) method with maximum-random overlap is used in the RRTMG to represent unresolved sub-grid clouds distribution.

The input variables required for the off-line RRTMG radiative transfer calculations include solar irradiance at the top of the atmosphere (TOA), ozone mixing ratio, trace gases mixing ratio (CO_2 and CH_4), air/surface temperatures, specific humidity, geopotential height, cloud amount, cloud liquid/ice water content, black carbon/ organic carbon/sulfate aerosol/sea salt/dust mixing ratio, surface albedo, surface latent/sensible heat flux. All of these fields are obtained from the MERRA-2 reanalysis product (Gelaro *et al* 2017) except for the trace gases mixing ratio, whose values came from the Copernicus Atmosphere Monitoring Service (CAMS) global inversion-optimized greenhouse gas concentrations (https://ads.atmosphere.copernicus.eu/cdsapp#!/dataset/cams-global-greenhouse-gas-inversion). MERRA-2 is the latest and first long-term global atmospheric reanalysis to assimilate aerosols observations and represent aerosol-climate interactions from the National Aeronautics and Space Administration (NASA), which well captures the temporospatial variations of aerosols over China compared to the ground measurements (Song *et al* 2018, Zhang *et al* 2020). It has a $0.5° \times 0.625°$ horizontal resolution with 42 pressure levels ranging from 1000 to 0.1 hPa, covering the period of 1980 to present. Note that the aerosols induced clouds changes are not separated in MERRA-2 as well as other reanalysis datasets, which cannot serve as an independent input in the CFRAM-A calculation to derive a contribution term of aerosol indirect effects. CAMS global inversion-optimized greenhouse gas concentrations have a $1.9° \times 3.75°$ horizontal resolution with 39 model levels from surface to TOA, covering the period 1979–2020, for CO_2 concentration. It has a $2° \times 3°$ horizontal resolution with 34 model levels from surface to TOA, covering the period 1990–2019, for CH_4 concentration. The quality-controlled (referred to Jiang *et al* 2019) *in-situ* observations of monthly ground surface temperature

in China for 1970–2019, compiled by the China Meteorological Administration (CMA), are used to verify the MERRA-2 results.

We consider the averaged winter (DJF) state of 2004/05-2018/19 as the base state (climate state '*A*' as discussed previously), and 2016/17 DJF averaged state as the contrast to the base state (climate state '*B*' as discussed previously). The number of assimilated observations in MERRA-2 doubled after 2002 to approximately 2 million per 6 h cycle, most of which are contributed by the A-train satellites (Gelaro 2017). Abundant observations assimilated in MERRA-2 could significantly improve the reanalysis quality and further reduce the uncertainties of model dependent fields such as clouds and aerosols, which are sensitive and crucial to assess the spatial patterns and magnitudes in attribution analysis. Therefore, we have chosen to use more accurate datasets covering a shorter period (2004/05-2018/19) rather than less accurate datasets covering a longer period, regarding similar results are obtained using 1995/96-2018/19 as the base state (figure not shown). In summary, the climatology of the most recent 15 years was selected as base state due to the availability of the high-quality reanalysis, a new era of historical climate simulations after 2005 in the phase 6 of the Coupled Model Intercomparison Project (CMIP6; Eyring *et al* 2016), and a rather 'clean' aerosol background without major volcanic eruptions.

3. Results

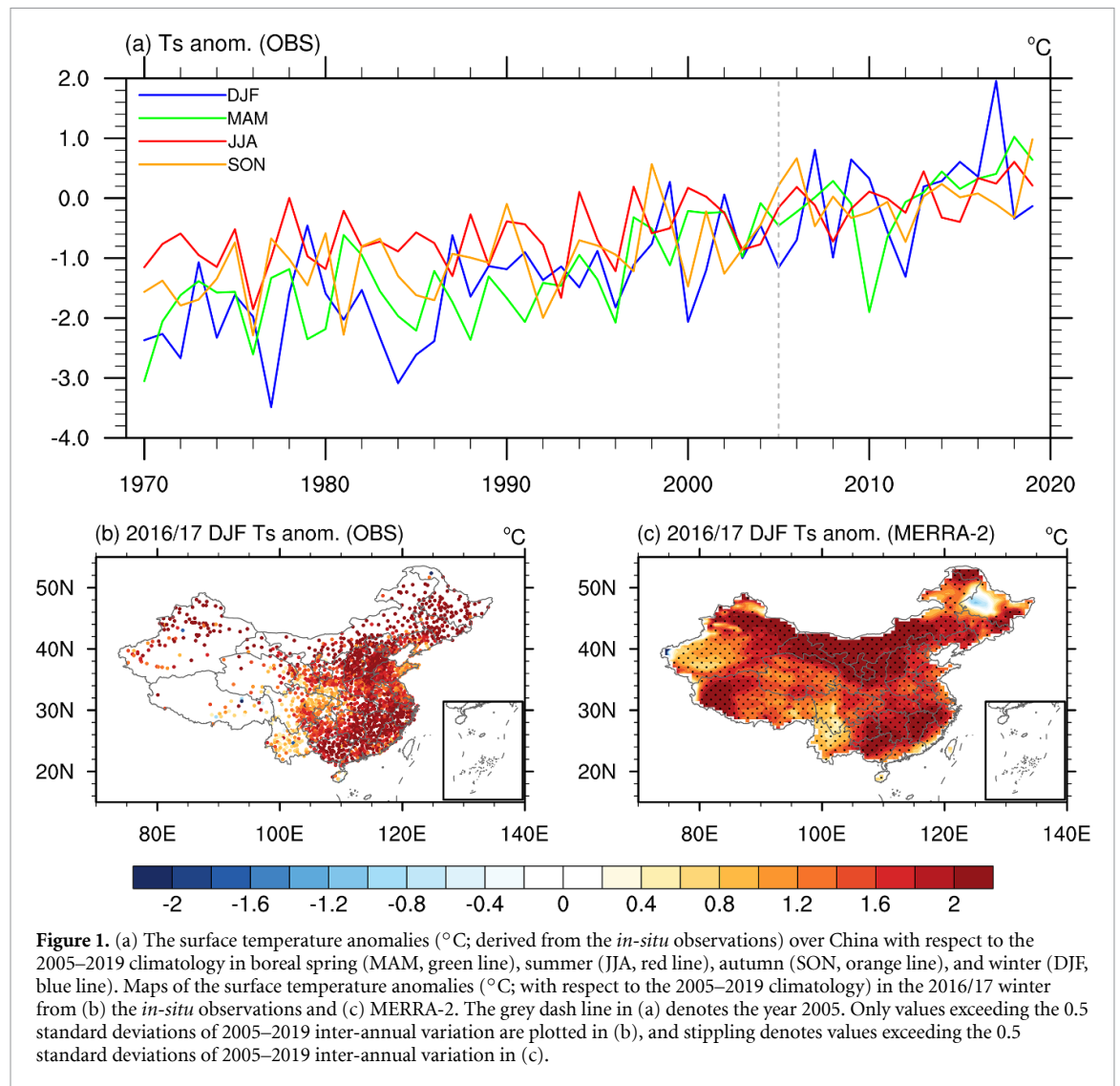## 3.1. Validation of the MERRA-2 quality and the CFRAM-A calculations

China has experienced an accelerated warming during the most recent decade, particularly in boreal winter (Li *et al* 2015, Qian and Zhang 2019, Xu *et al* 2020) (figure 1(a)). The most eye-catching warming occurred in the winter of 2016/17, with the surface temperature anomalies reaching the highest among recent years and seasons (figure 1(a)). Except for southwestern China, significant warm anomalies, defined as values exceeding the 0.5 standard deviation of the 2005–2019 winter mean temperature are observed almost throughout the country from the *in-situ* observations (figure 1(b)). Due to the different construction time of *in-situ* stations across the country, 2,133 stations were selected after quality control for the recent 15 years (2005–2019), while only 1,204 stations were selected for the 1970–2019 period in figure 1(a). Note that the similar results are obtained by using different sizes of stations for the two periods (figure not shown). MERRA-2 well captures the spatial pattern of surface warmings in the 2016/17 winter, including the prominent warming centers over northern and southeastern China and the mild warm anomalies over southwestern China (figure 1(c)). The high degree of consistency between MERRA-2 and

the observational data provide confidence to utilize this dataset as a proxy of observation for the subsequent analysis. A small patch of insignificant cold anomalies over northeastern China shown in MERRA-2 appears inconsistent with *in-situ* observations (figures 1(b) and (c)), and it is excluded from the subsequent attribution analysis.

To validate the CFRAM-A calculations, the surface temperature differences between the winters of 2016/17 and 2005–2019 base state derived from MERRA-2 and from summing the CFRAM-A derived partial temperature differences are presented in figures 2(a) and (b), respectively. The CFRAM-A calculation recovers the same spatial pattern as seen in the MERRA-2 (figures 2(a) and (b)). The area averaged surface temperature differences over China in MERRA-2 (1.61 K) and the CFRAM-A calculations (1.55 K) are quite close (figures 2(a) and (b)). Following Park *et al* (2012) and Chen *et al* (2017), the offline calculated radiative energy perturbations at the top of atmosphere (TOA) and the surface are validated through comparing with those in the MERRA-2 (figure not shown). The linearization errors are small at the surface, while positive biases are shown over western and central China at the TOA due to the linear solution tends to be very sensitive to the forcing in the stratosphere (Cai and Lu 2009). We focus on the surface temperature changes instead of the stratosphere temperature changes in this study. Therefore, the usage of time-mean fields in the offline radiative transfer calculations and the linearization of radiative energy perturbations in the CFRAM-A are reasonable.

3.2. The spatial structure of the process-based surface temperature attributions

With the CFRAM-A calculations validated, the derived partial surface temperature differences are used to quantify the relative contributions of individual physical and dynamical processes to the surface warming in the 2016/17 winter (figures 2(c)–(l)). Overall, the external forcings of solar irradiance and trace gases (ozone, CO_2, and CH_4) provide uniform warmings over China, which all induce less than 0.1 K area-averaged warmings (figures 2(c)–(f)). The processes associated with atmospheric dynamics, aerosols, and water vapor contribute most to the warming in 2016/17 winter, generating the area-averaged partial temperature differences of 0.98 K, 0.67 K, and 0.38 K, respectively (figures 2(l), (j), and (h)). More specifically, the water vapor anomaly, dominated by the longwave (i.e. 'greenhouse') effect, provides a remarkable warming across China expect the Tibetan Plateau (figure 2(h)), and this is clearly linked to the above-normal perceptible water in the 2016/17 winter (figure S1(c)). The surface temperature difference due to the changes in aerosol is primarily found over southeastern China (figure 2(h)). The effect of atmospheric dynamics is observed over most

Figure 1. (a) The surface temperature anomalies (°C; derived from the *in-situ* observations) over China with respect to the 2005–2019 climatology in boreal spring (MAM, green line), summer (JJA, red line), autumn (SON, orange line), and winter (DJF, blue line). Maps of the surface temperature anomalies (°C; with respect to the 2005–2019 climatology) in the 2016/17 winter from (b) the *in-situ* observations and (c) MERRA-2. The grey dash line in (a) denotes the year 2005. Only values exceeding the 0.5 standard deviations of 2005–2019 inter-annual variation are plotted in (b), and stippling denotes values exceeding the 0.5 standard deviations of 2005–2019 inter-annual variation in (c).

parts of China (figure 2(l)), which is likely linked to the weakening of large-scale cold air advection. This is supported by the positive phase of AO in the 2016/17 winter. This AO phase is associated with a weaker Siberian high and hence fewer episodes of cold surges affecting China (He *et al* 2017, Miao and Wang 2020). The weakening of the Siberian High also characterizes a weaker East Asian winter monsoon, which could lead to anomalous southerlies over China that were responsible for transporting more water vapor into land from adjacent ocean basins (Wu and Wang 2002). Although cloud changes provide an overall weak positive contribution to the warming (figure 2(i), 0.04 K), the effect is location sensitive with an obvious warming effect in southern China and cooling effect in central China. The cloud effects are dominated by its reflection of shortwave radiation and are directly related to changes in total cloud cover (figure S1(b)). The surface dynamics is mainly associated with negative feedbacks between the surface heat fluxes and temperature providing a strong cooling effect (−0.62 K) that is mostly seen over the warming center in southeastern China (figure 2(k)).

Surface albedo has an overall weak negative contribution to the warming (−0.04 K) with a significant local cooling effect in northeastern China and warming effect in the southwestern Tibetan Plateau that are directly linked to the local snow cover changes (figure S1(a). This result hints that the temperature bias in MERRA-2 over part of northeastern China is potentially caused by unrealistic representation of snow cover in MERRA-2. In summary, atmospheric dynamics and water vapor act as the main positive contributors to warming in northern China, compensated by the cooling effects of surface dynamics and clouds to some extent. In southeastern China, the warming is primarily attributed to the changes in atmospheric dynamics, aerosols, water vapor, and clouds, and is largely compensated by the cooling effect of surface dynamics. Unlike the other major contributors, which provide considerable effects in both northern and southern China, the aerosol effect is primarily concentrated over southern China.

The question is: Why the aerosol effect is crucial in southern China? To address this, we further decompose the total aerosol effect into partial

Figure 2. (a) The surface temperature differences (K) in winter between the 2016/17 and the 2005–2019 base state in MERRA-2, stippling denotes values exceeding the 0.5 standard deviations of 2005–2019 inter-annual variation. (b) The sum of partial surface temperature differences (K) derived from the CFRAM-A, and the partial surface temperature differences (K) due to changes in (c) solar irradiance, (d) ozone, (e) CO_2, (f) CH_4, (g) surface albedo, (h) water vapor, (i) clouds, (j) aerosols, (k) surface dynamics, and (l) atmospheric dynamics. The values on the upper right of the figure panels denote the area averaged values over China.

effects associated with five aerosol types (figure 3). The effects of anthropogenic aerosols (black carbon, organic carbon, and sulfate) contribute 90% of the area-averaged warming associated with the total aerosol change, particularly over southeastern China (figures 3(b)–(d)). The change in dust provides a uniform warming over China, and the effect of sea salt is almost negligible (figures 2(e) and (f)). Typically, all five types of aerosols reduce the surface temperature through scattering or absorption of incoming shortwave solar radiation (in general the direct effect) (Menon *et al* 2008, Najafi *et al* 2015). The aerosol-related net warming effect found by CFRAM-A is therefore linked to the reduction of aerosols in the 2016/17 winter in comparison to the 2005–2019 climatology, particularly over southeastern China (figure S1(d)). The dominant role of anthropogenic aerosols demonstrates that the reduction of aerosols likely comes from government regulations. Specifically, southeastern China has experienced the fastest urbanization and industrialization development in the last few decades, and it is also the
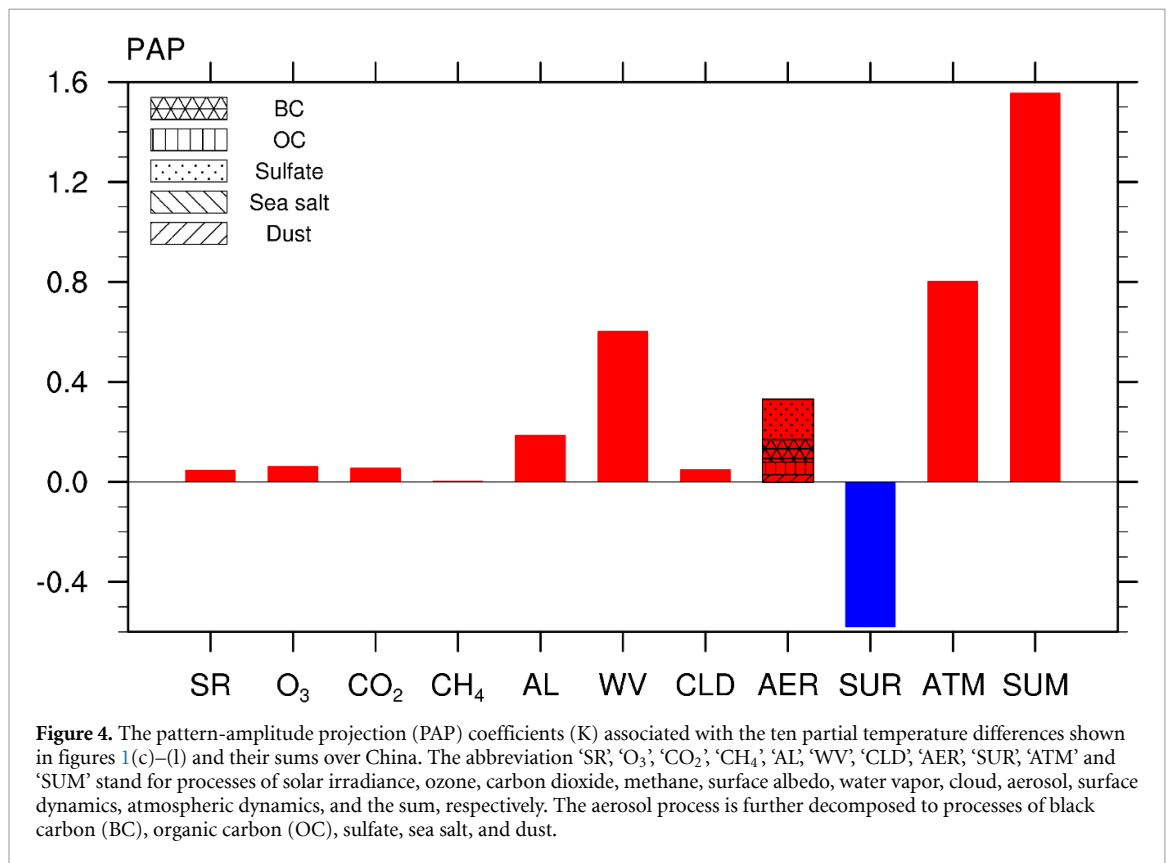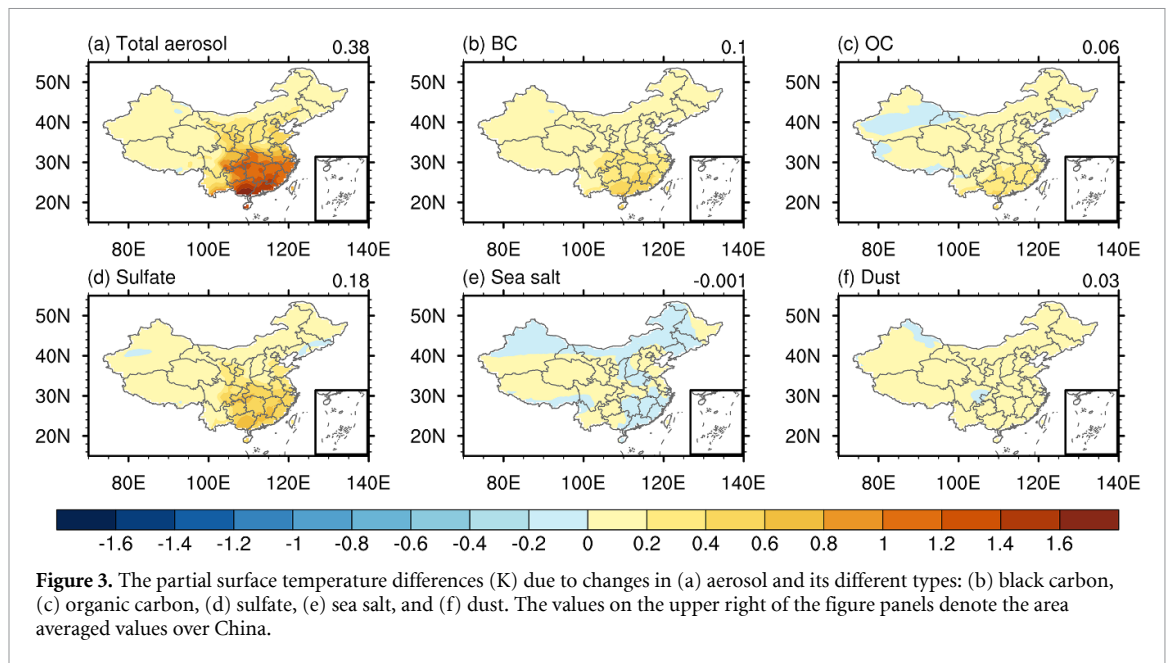
area with the most effective pollution reduction since the emission reduction policies were enforced in 2013 (Li *et al* 2018, Zheng 2018, Wei *et al* 2021).

3.3. Assessment of the overall contributions of individual processes to the surface temperature anomalies

Following Park *et al* (2012) and Deng *et al* (2013), a spatial 'pattern-amplitude projection' (PAP) coefficient is calculated to further quantify the overall contributions of individual processes to the spatial distribution of surface temperature anomalies over China in the 2016/17 winter. The PAP coefficient is defined as:

$$PAP_i = \langle \Delta T \rangle \times \frac{\Delta T_i \Delta T}{(\Delta T)^2}, \qquad (2)$$

where PAP_i and ΔT_i are the spatial PAP coefficient and partial surface temperature differences linked to the ith process, respectively. ΔT is the total surface temperature difference, and $\langle \rangle$ denotes the calculation of area average. The sum of all PAP_i equals to the

Figure 3. The partial surface temperature differences (K) due to changes in (a) aerosol and its different types: (b) black carbon, (c) organic carbon, (d) sulfate, (e) sea salt, and (f) dust. The values on the upper right of the figure panels denote the area averaged values over China.

Figure 4. The pattern-amplitude projection (PAP) coefficients (K) associated with the ten partial temperature differences shown in figures 1(c)–(l) and their sums over China. The abbreviation 'SR', 'O$_3$', 'CO$_2$', 'CH$_4$', 'AL', 'WV', 'CLD', 'AER', 'SUR', 'ATM' and 'SUM' stand for processes of solar irradiance, ozone, carbon dioxide, methane, surface albedo, water vapor, cloud, aerosol, surface dynamics, atmospheric dynamics, and the sum, respectively. The aerosol process is further decomposed to processes of black carbon (BC), organic carbon (OC), sulfate, sea salt, and dust.

area average of the total surface temperature differences shown in figure 2(b).

As expected, the three major positive contributors to the warming pattern are atmospheric dynamics, water vapor, and aerosols (figure 4). Although the change of surface albedo has an area-averaged net cooling effect (figure 2(g)), it provides a considerable positive contribution to the spatial pattern of warming. Changes of solar irradiance, ozone, CO$_2$, and clouds provide relatively smaller positive contributions to the spatial pattern while change of CH$_4$ shows a negligible impact. The only negative contributor is surface dynamics, which tends to cool the surface as the surface warms through transfer of sensible and latent heat to the atmosphere, providing negative feedback to surface temperature change.

4. Conclusion and discussion

The attribution of variations in surface temperature has attracted substantial interest and also generate lots of controversies within and beyond the climate community, especially with focuses now shifting from global to regional scales (Stott *et al* 2010, Najafi *et al* 2015, Zhai *et al* 2018). In this study, an updated CFRAM incorporating aerosol effects, namely the CFRAM-A, is developed and used to quantify the contributions from multiple radiative and dynamical processes responsible for the extreme warming over China in the 2016/17 winter.

The warming is observed throughout the country in this winter with remarkable warm anomalies over northern and southeastern China and relatively weak warm anomalies over southwestern China. The changes in atmospheric dynamics, water vapor, and aerosols contribute most to the magnitude and spatial structure of the warming. The effects of water vapor and atmospheric dynamics are detected over both northern and southeastern China, while the aerosol effect is primarily concentrated over southeastern China. The external forcings of solar irradiance, ozone, and CO_2 provide a moderate uniform warming throughout the country, while the effect of CH_4 is negligible. The effects of surface albedo and clouds are highly region-dependent. The surface albedo effect is important over high-latitudes or high-elevation regions, where significant snow cover changes are observed under global warming. The clouds effect is linked mainly to the regional total cloud cover changes, and to some degree includes indirect aerosol effects that cannot be isolated at this stage. The surface dynamics associated with negative feedbacks between the surface heat fluxes and surface temperature produces an overall cooling effect, compensating the warming in 2016/17 winter.

The CFRAM-A analysis reveals a considerable effect of warming associated with aerosols over southeastern China and this effect may ultimately be attributed to the effectiveness of emission reduction policies implemented in China since 2013 (Zhang *et al* 2018, 2019b, Zheng 2018, Zheng *et al* 2020, Wei *et al* 2021), given the dominant role of anthropogenic aerosols in the total aerosol effect. This finding suggests that mitigating pollution and reducing anthropogenic aerosols would accelerate regional warming, which likely occurred for Europe and North America after their emission reduction policies were issued in the last century (Ruckstuhl *et al* 2010, Turnock *et al* 2015, Yang *et al* 2018). It should be noted that this study only provides a preliminary quantitative attribution analysis of one extreme temperature case, and more comprehensive results will be obtained in the near future with additional cases and updated reanalysis datasets. One particular goal for the future work is to further constrain the effects of aerosols and clouds using ground-based and remote sensing observations.

Data availability statement

Acknowledgments

ORCID iDs

Tuantuan Zhang ⬥ https://orcid.org/0000-0002-1635-0625
Junwen Chen ⬥ https://orcid.org/0000-0001-8425-0880

References

Bony S *et al* 2006 How well do we understand and evaluate climate feedback processes *J. Clim.* **19** 3445–82

Cai M and Lu J 2009 A new framework for isolating individual feedback processes in coupled general circulation climate models. Part II: method demonstrations and comparisons *Clim. Dyn.* **32** 887–900

Cai W, Li K, Liao H, Wang H and Wu L 2017 Weather conditions conducive to Beijing severe haze more frequent under climate change *Nat. Clim. Change* **7** 257–62

Chen J, Deng Y, Lin W and Yang S 2017a A process-based assessment of decadal-scale surface temperature evolutions in the NCAR CCSM4's 25-year hindcast experiments *J. Clim.* **30** 6723–36

Chen J, Deng Y, Lin W and Yang S 2017b A process-based decomposition of decadal-scale surface temperature evolutions over East Asia *Clim. Dyn.* **51** 4371–83

Deng Y, Park T-W and Cai M 2012 Process-based decomposition of the global surface temperature response to El Niño in boreal winter *J. Atmos. Sci.* **69** 1706–12

Deng Y, Park T-W and Cai M 2013 Radiative and dynamical forcing of the surface and atmospheric temperature anomalies associated with the Northern annular mode *J. Clim.* **26** 5124–38

Duan A *et al* 2022 Sea ice loss of the Barents-Kara Sea enhances the winter warming over the Tibetan Plateau *npj Clim. Atmos. Sci.* **5** 26

Eyring V, Bony S, Meehl G A, Senior C A, Stevens B, Stouffer R J and Taylor K E 2016 Overview of the coupled model intercomparison project phase 6 (CMIP6) experimental design and organization *Geosci. Model Dev.* **9** 1937–58

Fang H, Qin W, Wang L, Zhang M and Yang X 2020 Solar brightening/dimming over China's mainland: effects of

atmospheric aerosols, anthropogenic emissions, and meteorological conditions *Remote Sens.* **13** 88

Filonchyk M, Yan H and Zhang Z 2019 Analysis of spatial and temporal variability of aerosol optical depth over China using MODIS combined dark target and deep blue product *Theor. Appl. Climatol.* **137** 2271–88

Gelaro R *et al* 2017 The modern-era retrospective analysis for research and applications, version 2 (MERRA-2) *J. Clim.* **30** 5419–54

Giorgi F, Bi X and Qian Y 2002 Direct radiative forcing and regional climatic effects of anthropogenic aerosols over East Asia: a regional coupled climate-chemistry/aerosol model study *J. Geophys. Res. Atmos.* **107** 4439

Gong H, Wang L, Chen W and Wu R 2021 Evolution of the east Asian winter land temperature trends during 1961–2018: role of internal variability and external forcing *Environ. Res. Lett.* **16** 024015

Gu Y, Liou K N, Xue Y, Mechoso C R, Li W and Luo Y 2006 Climatic effects of different aerosol types in China simulated by the UCLA general circulation model *J. Geophys. Res.* **111** D15201

He S, Gao Y, Li F, Wang H and He Y 2017 Impact of Arctic oscillation on the east Asian climate: a review *Earth Sci. Rev.* **164** 48–62

Hegerl G and Zwiers F 2011 Use of models in detection and attribution of climate change *WIREs Clim. Change* **2** 570–91

Held I M and Soden B J 2006 Robust responses of the hydrological cycle to global warming *J. Clim.* **19** 5686–99

Hu X, Cai M, Yang S and Sejas S A 2018 Air temperature feedback and its contribution to global warming *Sci. China Earth Sci.* **61** 1491–509

Hu X, Yang S and Cai M 2016 Contrasting the eastern pacific El Niño and the central pacific El Niño: process-based feedback attribution *Clim. Dyn.* **47** 2413–24

Iacono M J, Delamere J S, Mlawer E J, Shephard M W, Clough S A and Collins W D 2008 Radiative forcing by long-lived greenhouse gases: calculations with the AER radiative transfer models *J. Geophys. Res.* **113** D13103

Jian Y, Lin X, Zhou W, Jian M, Leung M Y T and Cheung P K Y 2020 Analysis of record-high temperature over southeast coastal China in winter 2018/19: the combined effect of mid- to high-latitude circulation systems and SST forcing over the North Atlantic and tropical Western Pacific *J. Clim.* **33** 8813–31

Jiang X, Zhang T, Tam C-Y, Chen J, Lau N-C, Yang S and Wang Z 2019 Impacts of ENSO and IOD on snow depth over the Tibetan Plateau: roles of convections over the western North Pacific and Indian Ocean *J. Geophys. Res.* **124** 11961–75

Jiang Y, Yang X-Q and Liu X 2015 Seasonality in anthropogenic aerosol effects on east Asian climate simulated with CAM5 *J. Geophys. Res. Atmos.* **120** 837–61

Jiang Z, Yang H, Liu Z, Wu Y and Wen N 2014 Assessing the influence of regional SST modes on the winter temperature in China: the effect of tropical Pacific and Atlantic *J. Clim.* **27** 868–79

Lashof D A and Ahuja D R 1990 Relative contributions of greenhouse gas emissions to global warming *Nature* **344** 529–31

Li C, Zhao T and Ying K 2015 Effects of anthropogenic aerosols on temperature changes in China during the twentieth century based on CMIP5 models *Theor. Appl. Climatol.* **125** 529–40

Li J, Jiang Y, Xia X and Hu Y 2018 Increase of surface solar irradiance across east China related to changes in aerosol properties during the past decade *Environ. Res. Lett.* **13** 034006

Li Z *et al* 2007 Aerosol optical properties and their radiative effects in northern China *J. Geophys. Res. Atmos.* **112** D22S01

Liao H, Chang W and Yang Y 2014 Climatic effects of air pollutants over China: a review *Adv. Atmos. Sci.* **32** 115–39

Liebmann B, Dole R M, Jones C, Blad? I and Allured D 2010 Influence of choice of time period on global surface temperature trend estimates *Bull. Am. Meteorol. Soc.* **91** 1485–92

Liu X, Ma P L, Wang H, Tilmes S, Singh B, Easter R C, Ghan S J and Rasch P J 2016 Description and evaluation of a new four-mode version of the modal aerosol module (MAM4) within version 5.3 of the community atmosphere model *Geosci. Model Dev.* **9** 505–22

Lu J and Cai M 2009 A new framework for isolating individual feedback processes in coupled general circulation climate models. Part I: formulation *Clim. Dyn.* **32** 873–85

Ma S, Zhu C, Liu B, Zhou T, Ding Y and Orsolini Y J 2018 Polarized response of East Asian winter temperature extremes in the era of Arctic warming *J. Clim.* **31** 5543–57

Menon S, Unger N, Koch D, Francis J, Garrett T, Sednev I, Shindell D and Streets D 2008 Aerosol climate effects and air quality impacts from 1980 to 2030 *Environ. Res. Lett.* **3** 024004

Miao J and Wang T 2020 Decadal variations of the east Asian winter monsoon in recent decades. *Atmos. Sci. Lett.* **21** e960

Najafi M R, Zwiers F W and Gillett N P 2015 Attribution of arctic temperature change to greenhouse-gas and aerosol influences *Nat. Clim. Change* **5** 246–9

Pan X, Wang W, Li T, Xin F and Yu J 2021 Cause of an extreme warm and rainy winter in Shanghai in 2019 *Int. J. Climatol.* **41** 4684–97

Park T-W, Deng Y and Cai M 2012 Feedback attribution of the El Niño–Southern Oscillation–related atmospheric and surface temperature anomalies *J. Geophys. Res. Atmos.* **117** D23101

Pincus R, Barker H W and Morcrette J-J 2003 A fast, flexible, approximate technique for computing radiative transfer in inhomogeneous cloud fields *J. Geophys. Res. Atmos.* **108** 4376

Qian C and Zhang X 2019 Changes in temperature seasonality in China: human influences and internal variability *J. Clim.* **32** 6237–49

Rodhe H 1990 A comparison of the contribution of various gases to the greenhouse effect *Science* **248** 1217–9

Ruckstuhl C, Norris J R and Philipona R 2010 Is there evidence for an aerosol indirect effect during the recent aerosol optical depth decline in Europe? *J. Geophys. Res. Atmos.* **115** D04204

Song Z *et al* 2018 Diurnal and seasonal variability of PM2.5 and AOD in North China Plain: comparison of MERRA-2 products and ground measurements *Atmos. Environ.* **191** 70–78

Stott P A, Gillett N P, Hegerl G C, Karoly D J, Stone D A, Zhang X and Zwiers F 2010 Detection and attribution of climate change: a regional perspective *WIREs Clim. Change* **1** 192–211

Sun Y, Zhang X, Ding Y, Chen D, Qin D and Zhai P 2021 Understanding human influence on climate change in China *Natl Sci. Rev.* **9** nwab113

Taylor P C, Ellingson R G and Cai M 2011 Geographical distribution of climate feedbacks in the NCAR CCSM3.0 *J. Clim.* **24** 2737–53

Tian Y *et al* 2012 Warming impacts on winter wheat phenophase and grain yield under field conditions in Yangtze Delta Plain, China *Field Crops Res.* **134** 193–9

Turnock S T *et al* 2015 Modelled and observed changes in aerosols and surface solar radiation over Europe between 1960 and 2009 *Atmos. Chem. Phys.* **15** 9477–500

Wei J *et al* 2021 Reconstructing 1-km-resolution high-quality PM$_{2.5}$ data records from 2000 to 2018 in China: spatiotemporal variations and policy implications *Remote Sens. Environ.* **252** 112136

Wetherald R T and Manabe S 1988 Cloud feedback processes in a general-circulation model *J. Atmos. Sci.* **45** 1397–416

Wu B and Wang J 2002 Winter Arctic oscillation, Siberian high and East Asian winter monsoon *Geophys. Res. Lett.* **29** 1897

Xiao D, Zuo Z, Zhang R, Zhang X and He Q 2018 Year-to-year variability of surface air temperature over China in winter *Int. J. Climatol.* **38** 1692–705

Xie J, Zhang M and Liu H 2019 Role of Arctic sea ice in the 2014–2015 Eurasian warm winter *Geophys. Res. Lett.* **46** 337–45

Xu C, Hou M, Yan X and Zhang X 2020 Temporal variability of seasonal warming rates in China *Int. J. Climatol.* **41** E1597–607

Yang X, Zhao C, Zhou L, Wang Y and Liu X 2016 Distinct impact of different types of aerosols on surface solar radiation in China *J. Geophys. Res. Atmos.* **121** 6459–71

Yang Y, Wang H, Smith S J, Zhang R, Lou S, Yu H, Li C and Rasch P J 2018 Source apportionments of aerosols and their direct radiative forcing and long-term trends over continental United States *Earth's Future* **6** 793–808

Yao T *et al* 2019 Recent third pole's rapid warming accompanies cryospheric melt and water cycle intensification and interactions between monsoon and environment: multidisciplinary approach with observations, modeling, and analysis *Bull. Am. Meteorol. Soc.* **100** 423–44

Yin Z, Wang H and Chen H 2017 Understanding severe winter haze events in the North China Plain in 2014: roles of climate anomalies *Atmos. Chem. Phys.* **17** 1641–51

You Q, Ren G, Fraedrich K, Kang S, Ren Y and Wang P 2013 Winter temperature extremes in China and their possible causes *Int. J. Climatol.* **33** 1444–55

Yu H, Luedeling E and Xu J 2010 Winter and spring warming result in delayed spring phenology on the Tibetan Plateau *Proc. Natl Acad. Sci.* **107** 22151–6

Zhai P, Zhou B and Chen Y 2018 A review of climate change attribution studies *J. Meteorol. Res.* **32** 671–92

Zhang G, Nan Z, Wu X, Ji H and Zhao S 2019a The role of winter warming in permafrost change over the Qinghai-Tibet Plateau *Geophys. Res. Lett.* **46** 11261–9

Zhang Q *et al* 2019b Drivers of improved $PM_{2.5}$ air quality in China from 2013 to 2017 *Proc. Natl Acad. Sci.* **116** 24463–9

Zhang T, Yue X, Li T, Unger N and Yang X 2018 Climate effects of stringent air pollution controls mitigate future maize losses in China *Environ. Res. Lett.* **13** 124011

Zhang T, Zang L, Mao F, Wan Y and Zhu Y 2020 Evaluation of Himawari-8/AHI, MERRA-2, and CAMS aerosol products over China *Remote Sens.* **12** 1684

Zhang X, Bai X, Hou M, Chen Z and Manzanedo R D 2019c Warmer winter ground temperatures trigger rapid growth of dahurian larch in the permafrost forests of Northeast China *J. Geophys. Res.* **124** 1088–97

Zhang Y, Qiu X, Yin T, Liao Z, Liu B and Liu L 2021 The impact of global warming on the winter wheat production of China *Agronomy* **11** 1845

Zheng B *et al* 2018 Trends in China's anthropogenic emissions since 2010 as the consequence of clean air actions *Atmos. Chem. Phys.* **18** 14095–111

Zheng Y, Zhang Q, Tong D, Davis S J and Caldeira K 2020 Climate effects of China's efforts to improve its air quality *Environ. Res. Lett.* **15** 104052

Zuo Z, Li M, An N and Xiao D 2022 Variations of widespread extreme cold and warm days in winter over China and their possible causes *Sci. China Earth Sci.* **65** 337–50

Zuo Z, Zhang R, Huang Y, Xiao D and Guo D 2015 Extreme cold and warm events over China in wintertime *Int. J. Climatol.* **35** 3568–81